Metrol. Meas. Syst., Vol. XXI (2014), No. 1, pp. 121–132.

PAN POLSKA AKADEMIA NAUK

METROLOGY AND MEASUREMENT SYSTEMS

Index 330930, ISSN 0860-8229

www.metrology.pg.gda.pl

M&MS

DESIGN AND TEST OF A NEW HIGH-CURRENT ELECTRONIC CURRENT TRANSFORMER WITH A ROGOWSKI COIL

Ming Zhang [1)] , Kaicheng Li [2)], Shunfan He [2)] , Jun Wang [1)]

1) Wuhan Textile University, School of Electronic and Electrical Engineering, Wuhan 430074, Hubei Province, China, (✉ zhangming@wtu.edu.cn)

2) Huazhong University of Science and Technology, School of Electrical and Electronic Engineering, Wuhan 430074, Hubei Province, China

Abstract

This paper describes the design and test of a new high-current electronic current transformer based on a Rogowski coil. For better performances, electronic current transformers are used to replace conventional electro-magnetic inductive current transformers based on ferromagnetic cores and windings to measure high-current on the high voltage distribution grids. The design of a new high-current electronic current transformer is described in this paper. The principal schemes of the prototype and partial evaluation results are presented. Through relative tests it is known that the prototype has a wide dynamic range and frequency band, and it can allow high accuracy measurements.

Key words: Rogowski coil, high-current, electronic current transformer, electrical measurements.

1. Introduction

Traditional current transformers (CTs) with a ferromagnetic core have been widely used in power systems because of their perfect technologies and high reliability. However, in many applications the use of traditional CTs can be limited by electrical characteristics. If transient non-sinusoidal primary high current is present on the conductor being measured, the ferromagnetic core can become magnetically saturated, and the distorted secondary signals will bring many difficulties to measurement and protection in power systems. Moreover, the CTs must be degaussed to remove any residual field before they can be used again.

Compared with the traditional CTs, Rogowski coil current transducers (RCCTs) have many merits because the absence of a ferromagnetic core virtually eliminates circuit loading and saturation concerns. Therefore, these transducers have been researched and designed to replace the traditional CTs [1–5]. They have an excellent transient response capability. Moreover, Rogowski coils can produce a safe low voltage (LV) output eliminating the hazards associated with misalignment and open secondary windings. In addition the variety of diameters and current ranges available allows the user to carry only one lightweight probe for a wide range of applications. So their use has increased very recently in applications of power electronics [6], relay protection, and power quality measurements [7] or transients [8–10].

Article history: received on Jun. 20, 2013; accepted on Dec. 04, 2013; available online on Mar. 15, 2014; DOI: 10.2478/mms-2014-0012.

At present electronic current transformers (ECTs) with a Rogowski coil have been developed, which bring simple insulation structures and excellent dynamic performances to electronic instrument transformers [11]. In this paper, a new high-current ECT with Rogowski coil is designed. In order to simplify the design of the equipment, the designed ECT consists of two parts: a high-voltage (HV) side unit and power supply unit. It is a key technology in application the optical transmission as the communication interface is used between the HV side unit and merging unit (MU). Relative tests will be carried out to reveal the merits of the designed ECT: high accuracy, good transient performance ect.

2. Electronic Current Transformer Design

2.1. Rogowski coil current transducer

The Rogowski coil is a coil distributed uniformly in a non magnetic core that surrounds the conductor carrying the current to be measured, as indicated in Fig. 1. The sensing coil consists of the wire group wound and internal return wire loop in the opposite direction. This arrangement ensures excellent suppression of external magnetic fields [12−14].

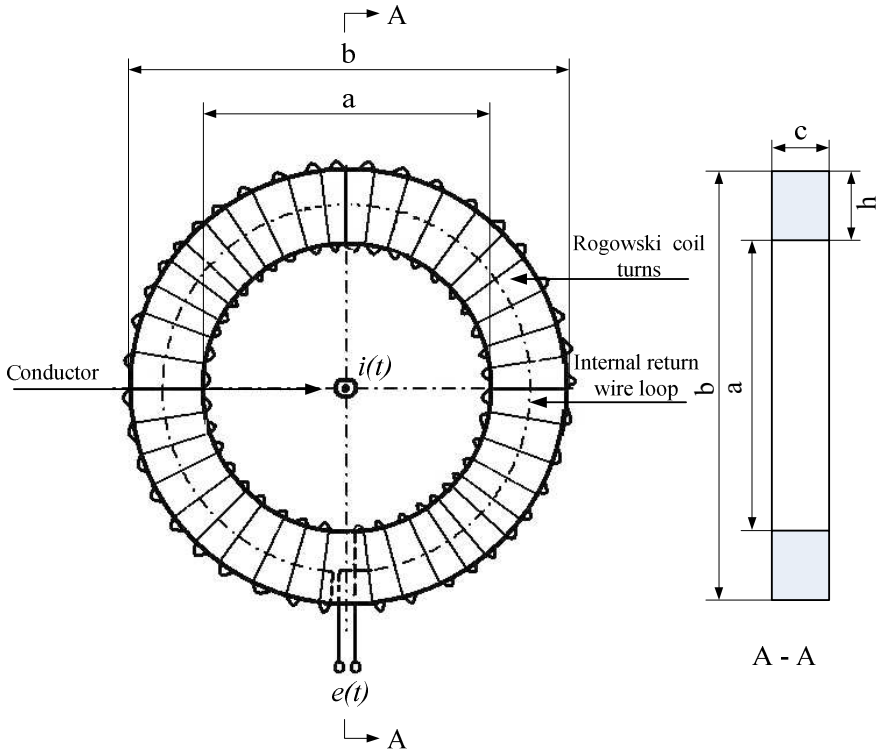

Fig. 1. Dimensions of the Rogowski coil.

If the current varies with time, a magnetic flux is produced in the coil and applying Faraday´s law of electromagnetic induction to the circuit of Fig. 1, we can obtain a voltage defined by

$$e(t) = -M\frac{di(t)}{dt}, \tag{1}$$

where M is the mutual inductance. The coil detects a voltage signal proportional to the change in the current passing through this conductor.

Table 1. Dimensions of the Rogowski coil.

Rogowski coil dimensions	Specifications
Inner diameter a	105 mm
Outer diameter b	135 mm
Section dimension of the core $h \times c$	15×10 mm
Diameter of the wire ϕ	0.25 mm
Number of turns N	1470

The construction of a Rogowski coil presents some difficulties, because for having some accuracy we need that the turns be equally distributed along the core and the return wire go back concentrically to avoid the external fields produced by external currents near the coil. For a toroidal coil having a circular cross section in Fig.1, the coil parameters can be analyzed and calculated. The dimensions of the Rogowski coil are given in Table 1. As shown in Fig. 2, we have built a Rogowski coil of 1470 turns of wire of 0.25 mm diameter. The coil with 21μH mutual inductance and 49Ω resistance is implemented to detect the current change with time.

Fig. 2. Physical aspect of the Rogowski coil.

The designed current transducer is expected to work in a HV environment and therefore the sensing part has to be galvanically separated from the signal processing part of the ECT. In this paper, the HV RCCT head mainly consists of a Rogowski coil, HV side circuit board and power supply module, as shown in Fig. 3.

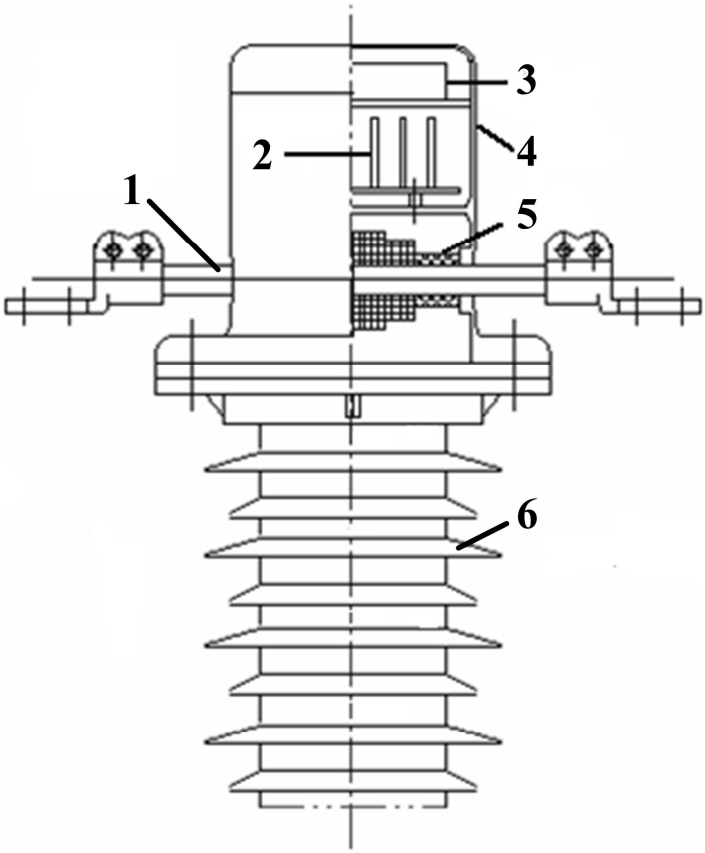

Fig. 3. Scenograph of the HV RCCT head:
1-conductor, 2-circuit board room,3-power source room,
4-tank, 5-coil room, 6-insulation sleeving.

2.2. Electronic Current Transformer Design

Optical fibers are well suited for transmission in HV environments by virtue of their all dielectric construction. They are highly resistant to electrical break-down and electromagnetic interference. Due to the working HV environment, the ECT is designed as two standalone units mutually interconnected only via the optical fiber. The principal diagram of the ECT is shown in Fig.4. The real-time data is sampled at the HV side unit and transferred through the optical fiber to the MU.

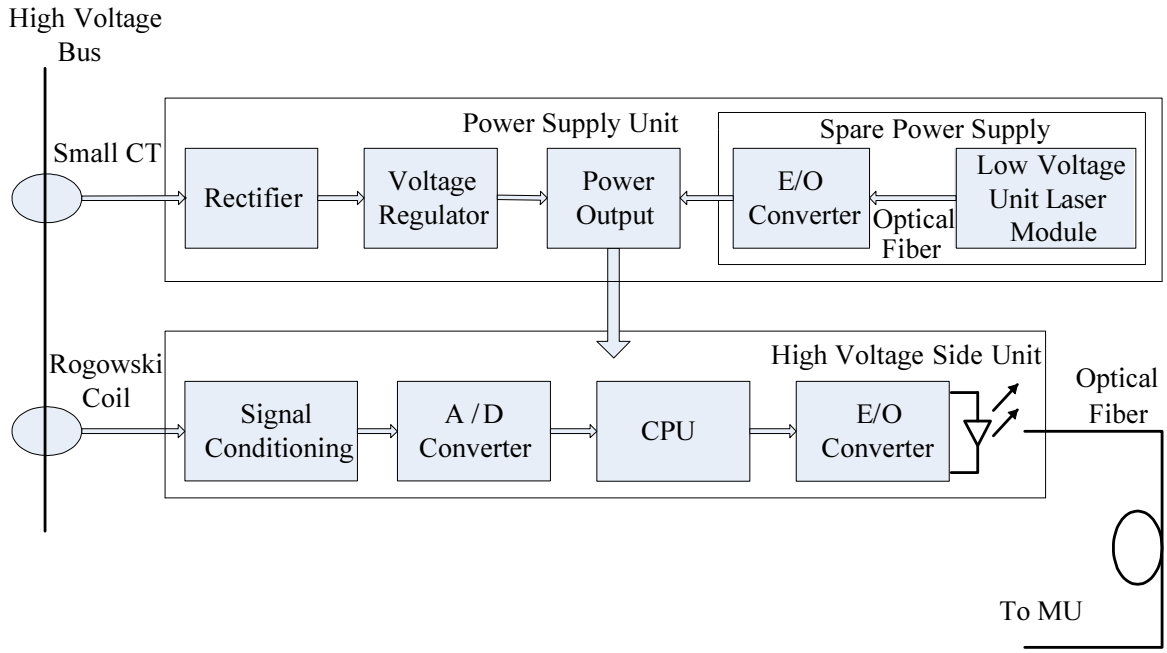

Fig. 4. Schematic diagram of the ECT with a Rogowski coil.

As shown in Fig.4, the HV side unit mainly includes front-end signal conditioning, an AD converter and microcontroller modules. Including an integrator, amplifier, low-pass filter, phase shift circuit, the signal conditioning module is designed using operational amplifiers with the appropriate bandwidth, as shown in Fig.5. For obtaining the original current wave shape we need to integrate the signal at the output of the Rogowski coil. The output is connected to an integrator and amplifier in order to provide an output signal that is proportional to the current in the primary conductor. Moreover, a 2-nd order low-pass filter can remove high frequency components which could result in aliasing and increased noise. And the phase shift circuit can compensate the phase error of the front-end circuit. This design ensures accuracy and dynamics of the whole current measurement chain determined principally by the parameters of the circuit.

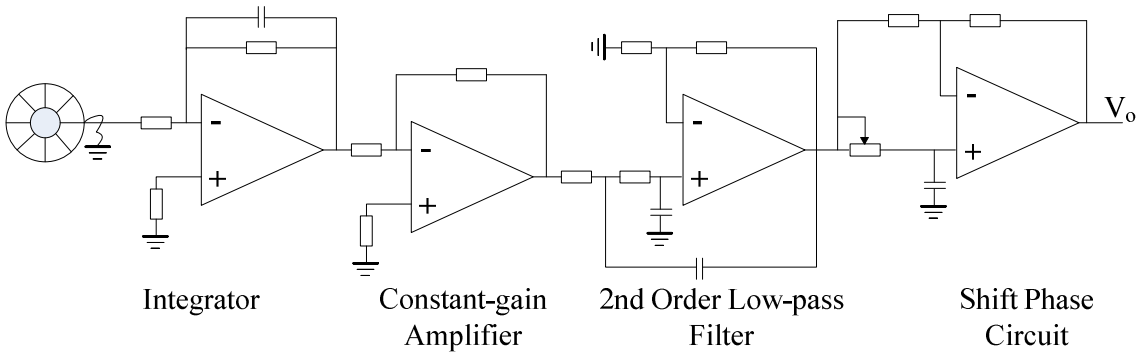

Fig. 5. Electronic circuit of the signal conditioning module.

For high accuracy and low power consumption, a MSP430F2419 is chosen to be the microcontroller, and an AD7685 is chosen for analog-to-digital (A/D) conversion. After receiving the trigger pulse, the CPU reads the data from A/D conversion through a serial peripheral interface (SPI), and then sends the data to the MU through a fiber optic transceiver HFBR-1414 (E/O converter). In order to reduce the number of the optical fibers needed for the transfer of data into the MU, the data is Manchester encoded. A HV side unit circuit board of the ECT was designed, as shown in Fig. 6.

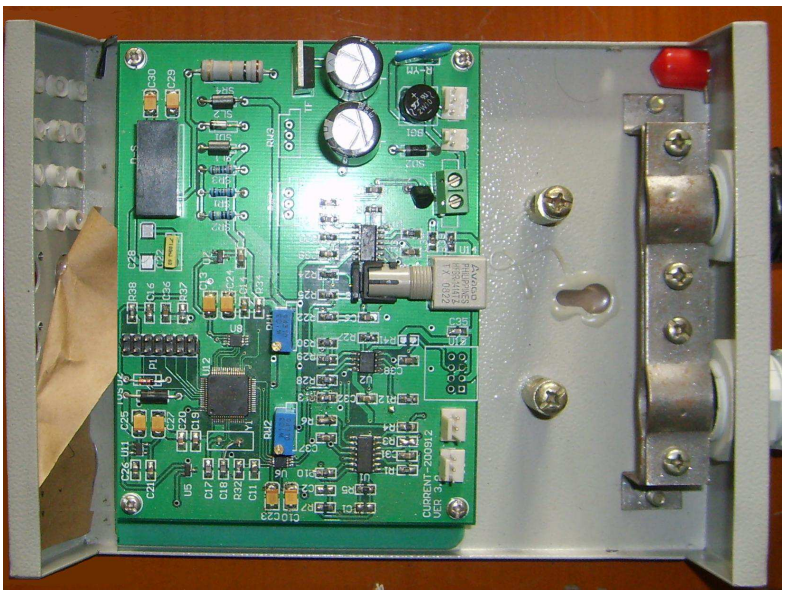

Fig. 6. The HV side unit circuit board of the ECT.

In the HV side unit, the integrator is located at the ground voltage level, so the electric power for ICs will be supplied directly from the small CT. However, this method of power supply may interrupt continuous measurement in case of power system malfunctions. As shown in Fig. 4, a second optical fiber is used to power the HV side unit. This fiber is fed by a laser emitter located on the LV side. The laser beam energy is converted into electrical energy in the HV side unit by means of a high- efficiency photovoltaic cell.

3. Testing

3.1. Test of the designed RCCT

In order to individually verify the designed RCCT, its accuracy can be measured in a large range of currents by comparing it with the standard CT with an accuracy of class ± 0.02% . The ratio error ε is defined as [15]

$$\varepsilon(\%) = \frac{K_r I_s - I_p}{I_p} \times 100 \,, \tag{2}$$

where K_r is the rated transformation ratio, I_p is the root-mean-square (RMS) value of the actual primary current, I_s is the RMS value of secondary current. The general definition for phase displacement is

$$\varphi(\text{rad}) = \varphi_s - \varphi_p, \tag{3}$$

where ϕ is the phase displacement, ϕ_p is the primary phase displacement, ϕ_s is the secondary phase displacement.

In the actual test, each data point was continuously sampled 20 times. The average measuring errors are shown in Fig.7 when the current changes within 5 ~ 120% of the rated current (50 ~1200A). As shown in Fig.7, the result shows that the designed RCCT with the integrator is perfectly meeting the requirement of class ±0.2% accuracy. But when the primary current is below 20% of the rated current, the output of the RCCT may be influenced by the low signal-to-noise ratio. Hence, the amplifier circuit and filter circuit are needed to adjust the output of the RCCT.

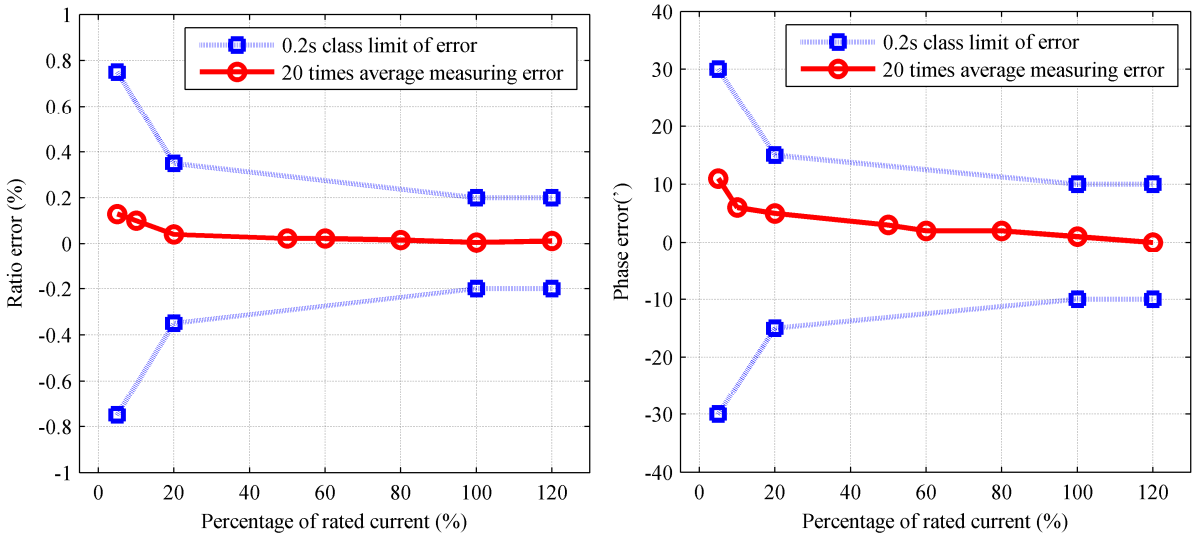

Fig. 7. (a) The normalized ratio error results of the designed RCCT tests.
(b) The normalized phase error results of the designed RCCT tests.

In fact, the DC components of transient currents may lead to deep saturation of the ferromagnetic core. Therefore, it will make the secondary output signal of the traditional CT distorted and disproportional to the primary current. But when compared with a ferromagnetic core sensor, Rogowski coils have no disadvantages like material saturation caused by high transient currents. So, it is desirable to design an available and feasible high transient current sensor .

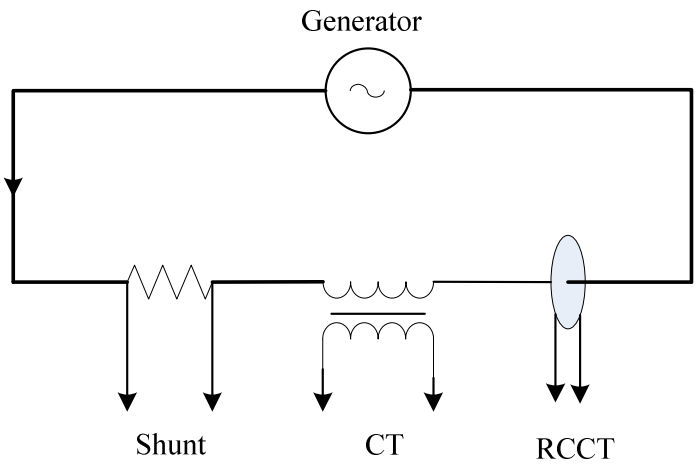

Fig. 8. Circuit connection for transient performance tests.

The transient performance of ECT mainly lies on that of the RCCT. With respect to the ability of the designed RCCT to detect transient currents, an experimental platform for dynamic simulation is set up as shown in Fig.8. A shunt (100μΩ), a CT (with class 0.2 accuracy) and the designed RCCT were connected in series. The short-circuit current of a generator was used to provide the transient current. In order to transfer the secondary current of CT and RCCT into a voltage signal, a 1Ω standard resistor and integrator were connected in the secondary circuit, respectively. Then, the output voltage waveforms of the test are recorded by the digital fault recorder, as shown in Fig.9.

The shunt has excellent transient performance and its output seems to be absolutely proportional to the high transient current with DC components. So the shunt is used as the criterion in the test. Fig.9 shows that the designed RCCT has excellent dynamic performances similar to the shunt, while the conventional CT has been saturated clearly by DC components and cannot reflect the transient current.

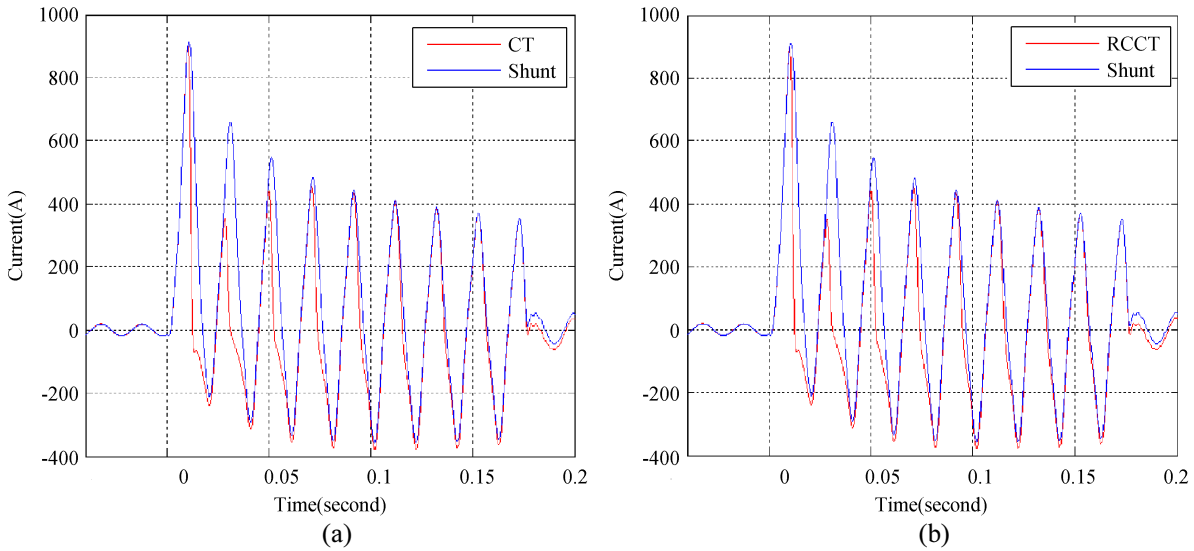

Fig. 9. (a) Waveforms of the CT and shunt. (b)Waveforms of the RCCT and shunt.

3.2. The test of the designed ECT

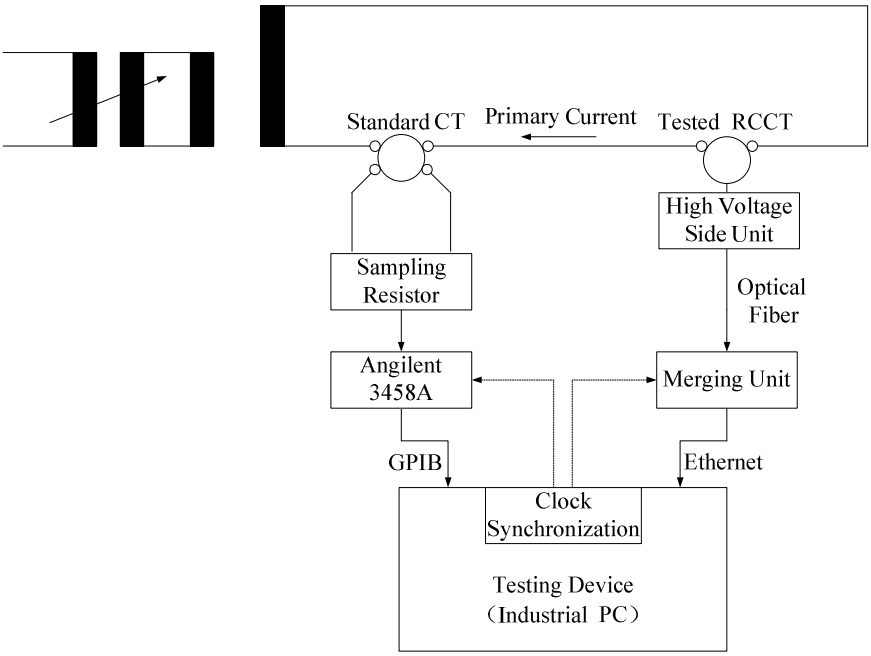

Fig. 10. Block diagram of the testing setup for verification of the ECT.

According to IEC60044-8, we have set up a test platform which is specified to estimate the measuring accuracy of the designed ECT. The block diagram of the test platform is shown in Fig.10 and the photos of the experimental setup are shown in Fig.11. It contains a reference channel, the tested channel and a testing device. The reference channel includes the standard CT (with class 0.02 accuracy), a sampling resistor (1Ω with class ± 0.012% accuracy), and an $8\frac{1}{2}$ digital multimeter (Agilent 3458A for analog-to-digital conversion). In the reference channel, the standard CT would provide an output current, and then through the standard resistor, Agilent's digital multimeter with data acquisition cards can provide the digital signal and ensure high accuracy. The tested channel includes the RCCT, HV side unit and MU. In the tested channel, the data from the RCCT is sampled in the HV side unit, then the sampling results are sent by the optical fiber to the MU. The data received from the reference and tested channels is sent to the industrial personal computer (IPC), which has the PCI-GPIB (General Purpose Interface Bus) Card and Ethernet interface. Using a self-developed clock synchronization card, the IPC transmits synchronous pulses to achieve synchronization of data acquisition. Then, the testing device based on the IPC begins receiving 10 cycles of data from the two channels and stores them in order. Finally, the calculations of the ratio error and phase error about two sets of data are made by using the FFT algorithm. For the testing device, Labview is used as the unified software platform for computing, storage, calling, and displaying on the IPC, which provides a convenient way for the present test system[16–19].

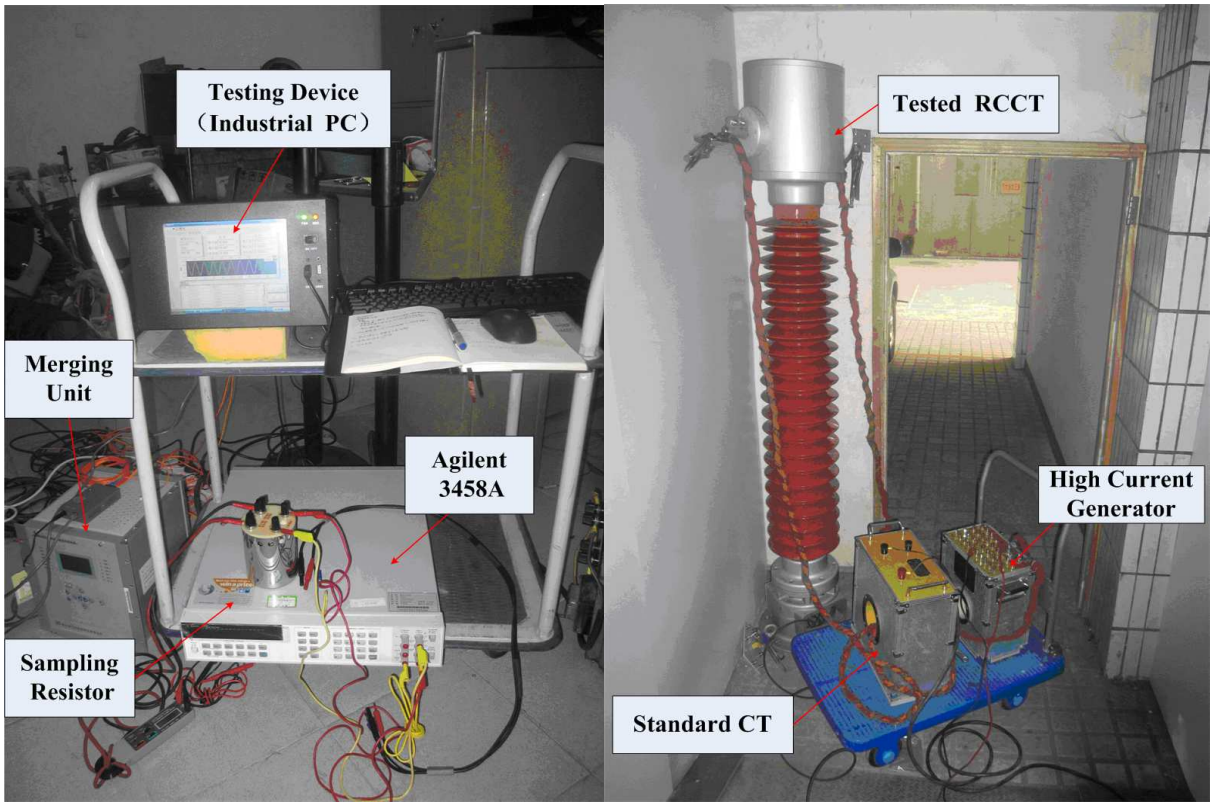

(a) (b)

Fig. 11. (a) Photo of the experimental setup of the standard CT and high-current generator.
(b) Photo of the experimental setup of the test platform.

As it is well known, actual power signals are not ideal. They can be considered as the sum of a series of different components superimposed over a fundamental component, and the amplitude of a harmonic is generally a few percent of that of the fundamental or smaller. With asynchronous sampling of the power signal, the application of the FFT algorithm for fundamental component spectral analysis will lead to inaccuracies due to the leakage effect, resulting in great ratio error of the test system. At the same time the spectral analysis precision of the harmonic components may also drop. In order to improve the resolution of spectral analysis, an improved algorithm based on combining the Hanning windowed interpolated FFT is proposed in this paper. An appropriate window function and interpolation algorithm can improve the calculation accuracy of FFT. It is insensitive to high frequency interference and frequency fluctuations of the measured signal. So, it has good stability and reliability [20].

In the actual test, 20 samples in each data point are adopted in the error calculation procedures. The test results are shown in Table 2 with a primary rated current of 1000A. According to IEC60044-8, current at 1%, 5%, 20%, 100%, 120% of the rated current must meet the accuracy requirements. Table 2 shows that the ratio error and phase error of the designed ECT are small and within the 0.2 S Class limit. So, the designed ECT can meet the accuracy requirements of 0.2 S Class standard.

Table 2. The ratio error and phase error of the designed ECT after averaging.

Percentage of rated voltage	Real percentage of rated voltage	Ratio error (%)	Phase error (')
1%	0.8%	0.18	14
	0.98%	0.17	13
	1.1%	0.19	10
5%	5.1%	0.13	9
	4.9%	0.10	7
	5.2%	0.12	5
20%	21%	0.1	3
	19%	0.09	3
	22%	0.08	2
100%	99%	0.04	1
	101%	0.04	0
	98%	0.06	1
120%	118%	0.03	0
	120%	0.04	1
	122%	0.02	1

4. Conclusions

A new high-current ECT with a Rogowski coil is presented in this paper. Galvanic separation of the HV side and LV side was achieved by using optical fibers for data and power transfer. So, the designed ECT can give good performance to meet the engineering demand for measuring the HV high-current. And the software realization with Labview shows low design costs and a short development cycle.

We have tested the designed ECT in order to improve its behavior and accuracy. It was characterized at 1%, 5%, 20%, 100%, 120% of the rated current by ratio error and phase error in two subranges. The designed ECT has achieved a high measurement accuracy, which meets the requirement of 0.2 S Class ECT.

The designed ECT can deal with both analog and digital signal outputs. It is not only suitable for existing conventional meters, but also can be fitted to digital meters with appropriate improvements. It has the following advantages: inherent electrical isolation; compact and light-weight construction, reduced installation and engineering costs, improved personal safety and good transient performance.

Acknowledgments

This work was supported by Natural Science Foundation of China grants 51077058 and 51277080.

References

[1] Chen, Q.; Li, H.; Huang, B.; Dou, Q. (2007). Rogowski sensor for plasma current measurement in J-TEXT. *IEEE Sensors J.*, 9(3), 293–296.

[2] Chen, Q.; Li, H.; Huang, B. (2010). An innovative combined electronic instrument transformer applied in high voltage lines.*Measurement*, 43(7), 960–965.

[3] Chiampi, M.; Crotti, G.; Morando, A. (2011). Evaluation of flexible Rogowski coil performances in power frequency applications. *IEEE Trans. Instrum. Meas.*, 60(3), 854–862.

[4] Cataliotti, A.; Cara, D. D.; Emanuel, E. A.; Nuccio, S.; Tinè, G. (2011). Characterization and error compensation of a Rogowski coil in the presence of harmonics. *IEEE Trans. Instrum. Meas.*, 60(4), 1175–1181.

[5] Djokic, V. B.; Ramboz, D. J.; Destefan, E. D. (2011). To what extent can the current amplitude linearity of Rogowski coils be verified. *IEEE Trans. Instrum. Meas.*, 60(7), 2409–2414.

[6] Kang, M. (1999). Analysis and design of electronic transformers for electric power distribution system. *IEEE Trans. Power Electron.*,14 (6), 1133–1141.

[7] Faifer, M.; Toscani, S.; Ottoboni, R. (2011). Electronic combined transformer for power-quality measurements in high-voltage systems. *IEEE Trans. Instrum. Meas.*, 60(6), 2007–2013.

[8] Liu, Y.; Lin, F.; Zhang, Q.; Zhong, H. (2011). Design and construction of a Rogowski coil for measuring wide pulsed current. *IEEE Sensors J.*, 11(1), 123–130.

[9] Zhang, Z.S.; Xiao, D.M.; Li, Y. (2009). Rogowski air coil sensor technique for on-line partial discharge measurement of power cables. *IET Sci., Meas. Technol.* , 3(3), 187–196.

[10] Poncelas, O.; Rosero, A. J.; Cusidó, J.; Ortega, A. J.; Romeral, L. (2009). Motor fault detection using a Rogowski sensor without an integrator. *IEEE Trans. Power Electron.* , 56(10), 4062–4070.

[11] Abdi-Jalebi, E.; McMahon, R. (2007). High-performance low-cost Rogowski transducers and accompanying circuitry. *IEEE Trans. Instrum. Meas.*, 56(3), 753–759.

[12] Ramboz, D. J. (1996). Machinable Rogowski coil, design, and calibration. *IEEE Trans. Instrum. Meas.*, 45(2), 511–515.

[13] Ferkovic, L.; Ilic, D.; Malaric, R. (2009). Mutual inductance of a precise Rogowski coil in dependence of the position of primary conductor. *IEEE Trans. Instrum. Meas.*, 58(1), 122–128.

[14] Marracci, M.; Tellini, B.; Zappacosta, C.; Robles, G. (2011). Critical parameters for mutual inductance between Rogowski coil and primary conductor. *IEEE Trans. Instrum. Meas.*, 60(2), 625–632.

[15] IEC60044-8 (2002). *Instrument Transformer-part 8, Electronic Current Transformers*. International Electrotechnical Commission: Geneva, Switzerland.

[16] Suomalainen, E.P.; Hallstrom, K.J. (2009). Onsite calibration of a current transformer using a Rogowski coil. *IEEE Trans. Instrum. Meas.*, 58(4), 1054–1058.

[17] Brandolini, A.; Faifer, M.; Ottoboni, R. (2009). A simple method for calibration for the traditional and electronic measurement current and voltage transformers. *IEEE Trans. Instrum. Meas.*, 58(5), 1345–1353.

[18] Draxler, K.; Styblikova, R.; Hlavacek, J.; Prochazka, R. (2011). Calibration of Rogowski coils with an integrator at high currents. *IEEE Trans. Instrum. Meas.*, 60(7), 2434–2438.

[19] Pan, F.; Chen, R.; Xiao, Y.; Sun, W. (2012). Electronic voltage and current transformers testing device. *Sensors*, 12(1), 1042–1051.

[20] Zhang,M.; Li,K.; Hu , Y. (2011). A high efficient compression scheme for power quality applications. *IEEE Trans. Instrum. Meas.*, 60(6), 1976–1985.